Eastern Mallard Adaptive Harvest Management Strategy, 2022

Anthony (Tony) Roberts, U.S. Fish and Wildlife Service, Atlantic Flyway Office, Patuxent National Wildlife Research Refuge, Laurel, MD, 20708

Jeffrey Hostetler, U.S. Fish and Wildlife Service, Atlantic Flyway Office, Patuxent National Wildlife Research Refuge, Laurel, MD, 20708

Joshua Stiller, New York Department of Environmental Conservation, Bureau of Wildlife, Albany, NY, 12233

Patrick K. Devers, U.S. Fish and Wildlife Service, Atlantic Flyway Office, Patuxent National Wildlife Research Refuge, Laurel, MD, 20708

William Link, U.S. Geological Service Eastern Ecological Center, Laurel, MD, 20708
Min Huang, Connecticut Department of Energy and Environmental Protection, Wildlife Division, Franklin, CT, 06254

G. Scott Boomer, U.S. Fish and Wildlife Service, Atlantic Flyway Office, Patuxent National Wildlife Research Refuge, Laurel, MD, 20708.

INTRODUCTION

Waterfowl harvest in the Atlantic Flyway has exhibited several characteristics that have differentiated it from harvest in other Flyways (Hawkins et al. 1984, Johnson et al. 2019). Prior to the 1980's the primary dabbling duck in the harvest was the American black duck (*Anas rubripes*), with other important species being wood ducks (*Aix sponsa*), mallards (*Anas platyrhynchos*), ring-necked ducks (*Aythya collaris*), and canvasback (*Aythya valisineria*). The mallard became one of the two primary ducks in the bag (along with wood ducks) around 1980. In 1995, general frameworks for all four flyways (Atlantic, Mississippi, Central, and Pacific) were based on the status of mid-continent mallards using the mid-continent mallard Adaptive Harvest Management strategy (MCM-AHM; USFWS 2019). The Atlantic Flyway Council (AFC) felt the MCM-AHM framework was not appropriate for setting the general duck season in the Atlantic Flyway because: 1) it did not represent the derivation of the Atlantic Flyway harvest;

2) did not account for the large mallard breeding population in the northeastern States and eastern Canada; 3) and exposed Atlantic Flyway hunters to potential restrictions resulting from the natural drought cycle of the mid-continent region.

An Eastern Mallard Adaptive Harvest Management (EM-AHM) Plan was developed and used to guide duck hunting seasons in the Atlantic Flyway from 1997 through 2018. This strategy addressed two concerns (2 & 3 above) that the Flyway had regarding the MCM-AHM framework, but it did not adequately account for the composition of harvest throughout the Flyway, particularly in the southern states. Reservations about the appropriateness of the EM-AHM framework for setting flyway regulations and concerns about the adequacy of the EM-AHM model to predict mallard dynamics lead the AFC to adopt a Multi-stock Adaptive Harvest Management strategy. This framework has been used since the 2019/20 migratory bird hunting season in the Atlantic Flyway to set general duck season regulations based on the status of four species; green-winged teal (*Anas crecca*), ring-necked duck, common goldeneye (*Buchephala clangula*), and wood duck (Johnson et al 2019, USFWS 2019).

Mallards are not represented in the suite of species used in Multi-stock AHM, but are still an important bird in the bag of AF hunters. Mallards in eastern North America have shown declining population trends over the last two decades, and hence a sustainable harvest strategy is needed to maintain the population while continuing harvest when warranted. The AFC decided to develop a single-species harvest strategy for eastern mallards. The fundamental objectives of the new strategy are to sustain an eastern mallard population that meets legal mandates (e.g., Migratory Bird Treaty Act) and provides consumptive and non-consumptive uses indefinitely. Relative to consumptive uses, the strategy is designed to maximize long-term harvest, maximize liberal hunting seasons, minimize closed seasons, and minimize annual regulatory changes. The

new strategy is predicated on an integrated population model (IPM) of eastern mallard population dynamics developed by the USFWS and Atlantic Flyway Technical Section. The objectives of the IPM are to accurately describe the annual demographics, determine the effect of harvest on annual survival and population growth, describe the effect of density dependence on annual population growth, and can be used with predictions in an optimization procedure to inform annual regulatory decisions.

METHODS

Study System

Eastern mallards are defined as the population of mallards breeding in the U.S. Atlantic Flyway, and in Canada east of 86 degrees longitude (Fig. 1).

Abundance Data

Mallard breeding population abundance in eastern North America is monitored using two surveys: 1) the Eastern Breeding Waterfowl Population and Habitat Survey (EBWPHS) and 2) the Atlantic Flyway Breeding Waterfowl Survey (AFBWS). The EBWPHS consists of a plot survey conducted by the Canadian Wildlife Survey (CWS) using helicopters (Bateman et al. 2017) and a transect survey conducted by the USFWS using fixed-wing aircraft (Smith 1995). A portion of the CWS plot surveys and USFWS transects overlap. These data are integrated using a hierarchical model to estimate total abundance in eastern Canada (Zimmerman et al. 2012). This estimate is known as the eastern composite estimate. In the Atlantic Flyway, a ground plot survey is used to estimate breeding waterfowl abundance from Virginia north to New Hampshire, USA (Heusmann and Sauer 1997, Heussmann and Sauer 2000). These data are analyzed in a Bayesian framework that accounts for time of day of the survey (Sauer et al. 2014).

The totals from the eastern composite estimate and the AFBWS are summed to obtain an eastern North America population estimate of mallards.

Mark-recovery Data

We estimated survival and harvest rates using data from banded and hunter recovered birds. Mallards were banded prior to the hunting season (i.e., pre-season; 1 July to 30 September; calendar years 1998-2018) and directly following the hunting season (i.e., post-season; 15 January to 31 March; calendar years 1999-2018) using standard protocols. We used all normal, wild-caught birds that were not fitted with auxillary markers (transmitters, nasal disks) and had no invasive procedures done (i.e. blood samples). All birds caught in the US Atlantic Flyway and Canada east of 86 degrees latitude were considered. Each bird was fitted with a standard U.S. Geological Survey leg band and the band number, sex, and age were recorded (Krapu et al. 1979, Carney 1992). During pre-season banding operations, birds were aged as hatch year (juvenile; age codes, 2, 3, 4) or after hatch-year (adult; codes 1, 7, 8). During post-season banding operations birds were aged as second year (juvenile; age code 5) or after second-year (adult; age code 6). We removed all post-season banded birds aged as after hatch year from our data set as those were an ambiguous age. We used encounters of banded birds that were shot or found dead (i.e., how obtained codes of 0 or 1) between September 1998 and January 2019.

Age Ratio Data

We used data from the USFWS and CWS Parts Collection Surveys (PCS), in combination with mark-recovery data, to estimate adjusted fall age ratios and differential vulnerability to harvest. The PCS survey provides information on the species, sex, and age composition of the annual harvest. We used all USFWS PCS records of mallards harvested in the Atlantic Flyway during

1998-2018 hunting seasons. We used CWS PCS records from Ontario, Quebec, and Atlantic Canada, 1998-2018.

Integrated Population Model

We developed a full annual cycle IPM to describe eastern mallard population demographics (Besbeas et al. 2002, Schaub et al. 2007, Hostetler et al. 2015, Arnold et al. 2018; Fig. 2). The IPM was composed of three subcomponent models: 1) annual and seasonal survival estimated using a Brownie dead recovery model. This model used pre- and post-season banding data of adults and juveniles to estimate age-specific harvest and seasonal survival rates (Brownie et al.1985); 2) a fecundity model using annual Parts Collection Survey data and banding and recovery data; and 3) a state-space model of the annual breeding abundance. We structured the IPM using available data during 1998-2018.

Survival sub-model and model selection.- We linked annual (S_t), cohort-specific (*ch;* adult male, adult female, juvenile male, and juvenile female), hunting season ($S^{h}_{ch,t}$; August-January) and non-hunting season ($S^{n}_{ch,t}$; February-August) survival using the Brownie H_7 model (Brownie et al. 1985, Devers et al. 2021). We estimated annual cohort-specific recovery ($f_{t,ch}$) probabilities from the Brownie H_7 model. We linked recovery to annual harvest rates ($h_{t,ch}$; using a vague prior probability distribution of beta(1,1)) and reporting rates (r_t) by

$$f_{t,ch} = h_{t,ch} \times r_t$$

We used year-specific values of mean reporting rates with associated standard deviations from work on the mid-continent population of mallards as prior information on r_t (G.S. Boomer personal communication). We then estimated kill rates ($K_{t,ch}$) using an estimate of crippling loss (c; 0.2; Anderson and Burnham 1976) as

$$K_{t,ch} = h_{t,ch} / (1\text{-}c)$$

Given uncertainties around mallard survival dynamics through time, we evaluated multiple structural forms of annual survival ($S_{ch,t}$) as a function of $S^{h}_{ch,t}$, $S^{n}_{ch,t}$, and $K_{t,ch}$ (Table 1). We ran each survival sub-model form on the mark-recovery data alone and calculated Watanabe-Akaike information criteria (WAIC; Watanabe 2010). WAIC is a more reliable estimator of Bayesian prediction information criterion (BPIC) than the widely used deviance information criterion, but unlike true leave-one-out cross-validation only requires running each model once (Gelman et al. 2014, Hooten and Hobbs 2015, Link and Sauer 2016). WAIC is computed on the likelihood of each data point, over the full posterior probability sample:

$$WAIC = -2\sum_{i=1}^{n} \log\left(\text{mean}^{s}\left(\Pr\left(y_i \mid \theta^{s}\right)\right)\right) + 2\sum_{i=1}^{n} \text{var}^{s}\left(\log\left(\Pr\left(y_i \mid \theta^{s}\right)\right)\right)$$

where n is the sample size, y_i is a single data point, and θ^s is posterior sample s of the model parameters. Therefore, the first term is the sum of the log of the likelihoods of each data-point, averaged over the full posterior probability sample, and the second term is the sum of the variances (over the full posterior probability sample) of the log-likelihoods of each data point. In the case of mark-recovery data, the data points are the outcomes of each release of a marked animal (either recovered in year t or not). There were two potential issues with estimating WAIC: amount of data and accuracy. With over 300,000 releases and 60,000 samples from the posterior probability, our dataset precluded standard methods for estimating WAIC. Therefore, we relied on the fact there are multiple data points that all have the same outcome (for example, there were 216 adult females banded pre-season in 1998 and recovered the same year):

$$WAIC = -2\sum_{o=1}^{O} n_o \log\left(\text{mean}^{s}\left(\Pr\left(y_o \mid \theta^{s}\right)\right)\right) + 2\sum_{o=1}^{O} n_o \text{var}^{s}\left(\log\left(\Pr\left(y_o \mid \theta^{s}\right)\right)\right)$$

where O is the number of outcomes with at least one data point, n_o is the number of data points with outcome o, and y_o is an example data point with outcome o. In this way, computing WAIC became tractable.

Under some circumstances, WAIC can fail to estimate BPIC accurately (Vehtari et al. 2017, Link et al. 2020). The R package loo contains functions that not only calculate WAIC and a similar estimator (PSIS-LOOIC; functions waic and loo, respectively) but also provide diagnostics on the reliability of each estimator (Vehtari et al. 2017). Due to the size of our dataset and posterior probability sample, we couldn't run these functions on the full set of data points. However, we determined that the results of the diagnostics for each data point with the same outcome would be the same. Therefore, we ran the waic and loo functions on the results of the model with a single data point standing in for each outcome with at least one data point (i.e. all 216 adult females banded pre-season in 1998 and recovered the same year were considered a single data point when testing model selection methodology). Both sets of diagnostics indicated no issues, and both WAIC and PSIS-LOOIC gave the same estimate of BPIC for the stand-in dataset. These results indicate that WAIC is a reliable model selection tool in this case.

The sub-model with the lowest WAIC value was used in the full IPM. All forms of the survival sub-model included a relationship with K to estimate the strength of cohort-specific additive harvest mortality on annual survival in the general form of:

$$S_t = a_{0,ch} * (1 - a_{1,ch} * K_{ch,t})$$

where a_0 was an intercept and a_1 was a measure of the additivity relationship. The estimation of cohort-specific S^h was the same in all models, where:

$$S^h_{t,ch} = 1 - K_{t,ch}$$

In addition, the estimation of cohort-specific S^n was the same in all models (Table 1), where:

$$S^n_{t,ch} = S_{t,ch} / S^h_{t,ch} \quad .$$

In all cases a_0 and the term for linear trend through time (a_3) were given vague normal priors (mean 0, variance 1000). The parameter a_1 was given a uniform prior constrained to 0-1. In this case 0 represents pure compensation and 1 pure additivity. We initially considered a logit-linear form of the annual survival model, but due to high WAIC values, relatively difficult formulation of some models, and the more traditional use of the linear form to represent partial compensation we did not include the logit-linear form in our model set. In all models we estimated cohort-specific seasonal non-hunting season survival for two periods. Survival from postseason banding to the spring population survey ($S^{wint}_{t,ch}$) and survival from the spring breeding survey to preseason banding ($S^{sum}_{t,ch}$) were estimated as:

$$S^{wint}_{t,ch} = S^{n\ 2/3}_{t,ch}$$
$$S^{sum}_{t,ch} = S^{n\ 1/3}_{t,ch}$$

Recruitment sub-model.- We estimated fall age ratios (juvenile female:adult female) using the ratio of juvenile female to total female wings in the PCS. The observed number of juvenile female wings was modeled as a binomial distribution from the total female wings. The proportion of juvenile female wings (prop.juv) was related to the true number of juveniles per adult in the harvest as:

$$\text{prop.juv} = AR^1 / 1 + AR^1$$

where AR^1 represented the age ratio uncorrected for differential vulnerability to harvest (DV). We corrected the age ratio for DV to get the corrected age ratio (AR) by:

$$AR^1 = AR * DV$$

The differential vulnerability was estimated as:

$$DV = \frac{\bar{f}_{t,JF}}{\bar{f}_{t,AF}}$$

thus linking mark-recovery data with PCS data. Finally, AR was modeled as a function of mallard population size and time as:

$$AR_t = c_0 - c_1 * N_t - c_2 * t$$

c_0 was the age ratio intercept, c_1 was the coefficient for population size, N is mallard abundance in year t, and c_2 was the coefficient for year, allowing for a time trend. All covariates in the recruitment sub-model were given a vague normal prior (mean 0, variance 1000) and in addition the c_1 parameter was truncated at 0 to not allow negative density dependence. The age ratio when used in the state-space model below assumes equal age ratios of juveniles at the time of banding, an assumption that has not been tested in the recently declining population.

State-space sub-model.- The breeding abundance estimate from surveys (observed) was modeled as the mean of latent abundance during spring with variance of the observed estimate. The spring population abundance was split between males and females and between adults and juveniles by multiplying by the proportion male and the proportion juvenile in the population respectively. The initial proportion of males in the population was given a uniform prior (0.5, 0.75) and the initial proportion of juveniles in the population was given a uniform prior (0.1, 0.8), and subsequent proportions were calculated from the annual sex- and age-specific estimates from the model.

We estimated latent cohort-specific (adult male [AM], adult female [AF], juvenile male [JM], and juvenile female [JF]) population sizes through the annual cycle (breeding [spr], post-breeding [fall], and post-hunting season [wint]; Figure 2). We assume the female sex ratio is equal to the male sex ratio when using AR_t in the model. The life-cycle model transitions juveniles to adults after the breeding season, directly before pre-season banding operations to match with the annual juvenile survival estimate from pre-season banding. We estimated the finite annual population growth rate ($\lambda_t = N_{t+1}/N_t$; >1.0 = increase; 1.0 = no change; <1.0 = decrease) as the latent breeding season population change over one year.

Model implementation.- We estimated posterior parameter distributions using Markov Chain Monte Carlo methods in JAGS (Plummer 2003) with the jagsUI package (Kellner 2019) for Program R (R Version 3.4.2, www.r-project.org, accessed 15 Jan 2018). We considered the Gelman statistic $\hat{R}$ with values <1.1 as indicative of adequate model convergence (Gelman and Hill 2007). We calculated Bayesian p-values for each of the sub-models within the IPM (Kéry and Royle 2016, Conn et al. 2018). If Bayesian p-values are too close to 0 or 1, it indicates lack of fit or unreasonably good fit. Although Bayesian p-values can be biased towards 0.5, they are a widely used, generally accepted, and informative test of fit. We also calculated $\hat{c}$ another fit statistic that estimates the magnitude of lack of fit. When $\hat{c}$ is greater than 1, it suggests overdispersion of the data compared to the model, although values less than 3 or 4 can be corrected for, if the cause of lack of fit truly is overdispersion (Burnham and Anderson 2002). To quantify the strength of the contribution of temporal variation in demographic parameters to variation in λ_t, we calculated the correlation between model parameters and λ_t using all Markov Chain Monte Carlo posterior estimates and function cor from the stats package. We also calculated the probability that the correlation was greater than 0.

Population dynamics.- We used the resulting model estimates to calculate equilibrium dynamics of the harvested eastern mallard population. We used the estimate of survival from the final year and beta parameters from the IPM in the model to find the optimum harvest rate for each population size, i.e. the harvest rate that resulted in a stable population, and ultimately maximum sustainable yield. For each harvest rate over a range (0–1 by 0.001), we used the optimize function in Program R to estimate the breeding population abundance that eastern mallards would equilibrate at by calculating the one-year change in abundance that was closest to 0. The harvest rate that resulted in the highest total harvest was considered the equilibrium harvest rate, or the harvest rate at maximum sustainable yield. The resulting harvest rate is the harvest rate on the spring breeding abundance, so we corrected the harvest rate to account for average reproductive rate to get the equilibrium harvest rate of the fall flight (breeding abundance plus reproduction minus mortality). The harvest rate was adjusted up by c to get an equilibrium K (kill rate).

Optimization routine

We used MDPSolve in MATLAB to explore how sets of harvest packages (regulations) would affect equilibrium dynamics of eastern mallards and the selection of individual harvest packages through time. We estimated the distribution of harvest rates at various bag limits, all with a 60-day season length to correspond with the season length of the general duck season during liberal seasons set by multi-stock AHM. Regulations we examined were:

- Closed, restrictive (1 bird bag), moderate (2), and liberal (4)
- Closed, restrictive (2 bird bag), moderate (3), and liberal (4)
- Closed, standard (2 bird bag), and liberal (4)
- Closed, restrictive (2 bird bag), moderate (4), and liberal (6)

All bag limits of 1, 2, or 3 also had a 1 hen mallard restriction and bag limits of 4 or 6 had a 2 hen mallard restriction.

For all population and model parameters we used the distribution (95% credible interval) of the parameter from the final model. Year was set to 2018 so as not to assume a continuing trend and uncertainty was included around the population and cohort-specific additivity estimates. We included a 98% of maximum sustainable yield (right shoulder) constraint and optimized for total harvest without a discount factor, similar to other AHM strategies. The optimum policy for each package was then used with the population model to simulate the response of eastern mallard abundance over 100 years with 1000 simulations. Summary statistics were derived including percent of time in each package (bag limit), the average fall flight, average harvest, percent of time the package was different from the previous year, average number of years between package changes, and the minimum breeding abundance.

RESULTS

Annual observed population estimates ranged from 1,421,000 in 1998 to 1,066,000 in 2018, with a negative trend over the entire time series (Table S1, Fig. 3). During 1998-2018, 91,147 adult and 196,909 juvenile mallards were banded during preseason, with an average of nearly 14,000 total mallards banded each year. Postseason banding 1999-2018 yielded 8,567 adults and 9,457 juveniles total, an average of just over 900 mallards per year. The total female mallard wings submitted annually ranged from 3,743 in 2000 to 1,773 in 2015 (Table S1).

We tested five forms of the survival sub-model. The top model included a juvenile trend in annual survival, followed by a hockey-stick trend in juvenile survival with a difference in WAIC from the top model of 0.5 (Table 1). We choose the top model for use in the IPM. The top three models all included a trend on juvenile survival, lending credibility to the hypothesis that

juvenile survival is actually declining. When the top survival sub-model was used in the IPM, fit statistics for all sub-models showed some signs of lack of fit (Table 2). Evidence for lack of fit was highest in pre- and post-season juvenile banding data.

The IPM posterior estimates for population abundance tracked closely with the observed estimates (Fig. 3). Posterior median estimates ranged from 1,039,000 in 2018 to 1,483,000 in 2000. The estimates did not decrease every year as in the observed values until about 2007. IPM posterior median estimates of mean annual growth rate over the period 1998-2018 ranged from 0.88 in 2000 to 1.08 in 2001. Average population growth rate over the entire time period (geometric mean) was 0.99 (95% credible interval 0.98-1.00). IPM posterior median estimates of annual and seasonal survival rates were relatively stable for adult cohorts and declined through time for juvenile cohorts (Table 3, Fig. 4). Harvest rates were stable for all cohorts in the last 10 years (Table 3). The additivity parameter had a wide credible interval for all cohorts and was similar between adult cohorts (95% credible intervals for male = 0.24-0.96 and female = 0.14-0.99) and between juvenile cohorts (male = 0.02-0.75, female = 0.04-0.97; Fig. 5). The time trend on annual juvenile survival had a 95% credible interval 0.014-0.032. Posterior median estimates of annual age ratios ranged from 0.74 juvenile females per adult female in 2000 to 1.06 in 2006 (Table 3). The age ratio density dependent effect (*c1*) was 0.001-0.003, and the time trend (*c3*) was 0.019-0.064. Annual growth rate was positively correlated with the female age ratio (Fig. 6). Finite population growth rate was not correlated with adult female survival or harvest rates or with juvenile female survival or harvest rates.

The results of the equilibrium analysis suggested a population abundance (during spring breeding) at maximum sustainable yield of 792,000 with a carrying capacity of 1,347,000. The

equilibrium population abundance would be reached at an equilibrium kill rate (pooled across cohorts) on the fall flight of 0.19.

Simulation of the optimal policy of the alternative regulatory structures resulted in similar characteristics (Table 4). The average fall flight ranged from a minimum of 1.53 to a maximum of 1.64 million mallards (a 7% difference). The mean minimum breeding abundance ranged from 930,000 to 990,000 (a 6% difference). The mean number of years between regulatory changes ranged from 3–5 years. The first three alternatives (with a maximum of 4-bird daily bag limit) produced optimal policies that were most frequently in the liberal 4-bird regulation (79-87%) with the 2-bird bag occurring in 13%-21% of the time. The most frequent alternative selected under the most liberal structure (2/4/6 bird bag limits) was the 2-bird bag (84%); the 6-bird bag regulation was selected 15% of the time. The 4-bird bag limit never occurred in the 2/4/6 regulatory structure. The 2/3/4 regulatory structure displayed results that were inconsistent with the 1/2/4 and 2/4 structures; the 2/3/4 structure never resulted in the implementation of the 3-bird bag regulatory alternative, but had an increased frequency of the 2-bird bag and a decreased frequency of the 4-bird bag. The 2/3/4 structure had the highest frequency of annual regulatory change (41%) and the 1/2/4 structure had the lowest frequency of changes (19%). The 1/2/4, 2/3/4, and 2/4 structures had optimal policies that called for the 4-bird bag alternative at the most recent observed breeding population abundance of 1.05 million birds (Fig. 7) and never employed the moderate package (e.g., 2- or 3-bird bag).

FINAL POLICY DECISIONS

On 24 February, 2022 the Atlantic Flyway Technical Section passed a recommendation for consideration by the Council to: 1) use the integrated population model as the analytical framework to derive annual harvest recommendations, 2) use of a 98% maximum sustained yield

with no constraints as the optimization objective, and 3) employ three regulatory alternatives (i.e., restrictive, moderate, and liberal) with season length established by the Atlantic Flyway Multi-stock Adaptive Harvest Management strategy. The daily bag limit under each regulatory alternative (restrictive, moderate, and liberal) in the recommendation was 1, 2, and 4 with corresponding hen restrictions of 1, 1, and 2. The Atlantic Flyway Council approved the recommendation at their 14 March, 2022 meeting. Here we outline the policy decisions and annual process for setting the bag limit of mallards in the Atlantic Flyway, within the general duck season frameworks derived from Multi-stock Harvest Management.

Annual Process

Each year the IPM will be updated with current year's data, including the most recent breeding population estimates, banding data from the previous pre- and post-season bandings and hunting recoveries, and previous hunting season PCS data. The resulting estimates of model parameters will be used in the optimization procedure. Harvest rates associated with each bag limit will be updated annually using Bayesian updating methods. The annual policy matrix will be derived with a constraint of 98% maximum sustainable yield. The model parameters estimated in year t will be used along with the selected bag limit for year t to develop a policy matrix for the hunting season in year t+1. In the event of reduced season length based on the general duck season, eastern mallard bag limits will follow the recommendation from the policy matrix (no substitution rules). The resulting matrix will be presented to the Atlantic Flyway within the annual USFWS Adaptive Harvest Management Report.

LITERATURE CITED

Anderson, D.R., and K.P. Burnham. 1976. Population ecology of the mallard: VI. The effect of exploitation on survival. U.S. Fish and Wildlife Service Resource Publication 128, Maryland, USA.

Arnold, T.W., R.G. Clark, D.N. Koons, and M. Schaub. 2018. Integrated population models facilitate ecological understanding and improved management decisions. Journal of Wildlife Management 82:266-274.

Bateman, M. C., D. Bordage, R. K. Ross, B. Collins, C. Lepage, S. Gilliland, R. C. Cotter, and K. M. Dickson. 2017. Helicopter-based waterfowl breeding pair survey in eastern Canada, 1990–2003. Pages 5–46 in D. Bordage, M. C. Bateman, R. K. Ross, and C. Lepage (eds.). Helicopter-based waterfowl breeding pair survey in eastern Canada and related studies. BDJV Special Publication. 236 pages.

Besbeas, P., S.N. Freeman, B.J. Morgan, and E.A. Catchpole. 2002. Integrating mark–recapture–recovery and census data to estimate animal abundance and demographic parameters. Biometrics 58:540–547.

Brownie, C., D.R. Anderson, K.P. Burnham, and D.S. Robson. 1985. Statistical inference from band recovery data: a handbook. U.S. Fish and Wildlife Service Resource Publication 131. Washington, D.C. 305pp.

Burnham, K.P. and D.R. Anderson. 2002. Model selection and multimodel inference: a practical information-theoretic approach. Springer Verlag, New York, NY, USA.

Carney, S. M. 1992. Species, age, and sex identification of ducks using wing plumage. US Department of the Interior report 144 pgs.

Conn, P. B., D. S. Johnson, P. J. Williams, S. R. Melin, and M. B. Hooten. 2018. A guide to Bayesian model checking for ecologists. Ecological Monographs 88:526–542.

Devers, P. K., R. L. Emmet, G. S. Boomer, G. S. Zimmerman, and J. A. Royle. 2021. Evaluation of a two-season banding program to estimate and model migratory bird survival. Ecological Applications 31.

Gelman, A. and J. Hill. 2007. Data analysis using regression and multilevel/hierarchical models. Cambridge University Press, New York, USA.

Gelman, A., J. Hwang, and A. Vehtari. 2014. Understanding predictive information criteria for Bayesian models. Statistics and computing 24:997–1016.

Hawkins, A.S., R.C. Hanson, H.K. Nelson, and H.M. Reeves, editors. 1984. Flyways: pioneering waterfowl management in North America. U.S. Government Printing Office, Washington, D.C., USA.

Heusmann, H.W. 1991. The history and status of the mallard in the Atlantic Flyway. Wildlife Society Bulletin 19:14-22.

Heusmann, H. W. and J. R. Sauer. 1997. A survey for mallard pairs in the Atlantic Flyway. Journal of Wildlife Management 61:1191-1198.

Heusmann, H. W. and J. R. Sauer. 2000. The northeastern states' waterfowl breeding population survey. Wildlife Society Bulletin 28:355-364.

Hooten, M. B., and N. T. Hobbs. 2015. A guide to Bayesian model selection for ecologists. Ecological monographs 85:3–28.

Hostetler, J. A., T.S. Sillett, and P.P. Marra. 2015. Full-annual-cycle population models for migratory birds. The Auk 132:433–449.

Johnson, F.A., G.S. Zimmerman, M.T. Huang, P.I. Padding, G.D. Balkcom, M.C. Runge, and P.K. Devers. 2019. Multi-species duck harvesting using dynamic programming and multi-criteria decision analysis. Journal of Applied Ecology 56:1447-1459.

Kellner, K. 2019. Package "jagsUI". https://cran.r-project.org/web/packages/jagsUI/index.html.

Kéry, M., and J. A. Royle. 2016. Applied Hierarchical Modeling in Ecology: Analysis of distribution, abundance and species richness in R and BUGS: Volume 1: Prelude and Static Models. Academic Press.

Krapu, G. L., D. H. Johnson, and C. W. Dane. 1979. Age determination of mallards. Journal of Wildlife Management 43:384–393.

Link, W. A., and J. R. Sauer. 2016. Bayesian cross-validation for model evaluation and selection, with application to the North American Breeding Bird Survey. Ecology 97:1746–1758.

Link, W. A., J. R. Sauer, and D. K. Niven. 2020. Model selection for the North American Breeding Bird Survey. Ecological Applications 30:e02137.

Plummer, M., 2003. JAGS: A program for analysis of Bayesian graphical models using Gibbs sampling. Pages 1-10 *in* K. Hornik, F. Leisch, and A. Zeileis, editors. Proceedings of the 3rd international workshop on distributed statistical computing (DSC 2003). Vienna, Austria.

Sauer, J. R., G. S. Zimmerman, J. D. Klimstra, and W. A. Link. 2014. Hierarchical model analysis of the Atlantic Flyway Breeding Waterfowl Survey. Journal of Wildlife Management 78:1050–1059.

Schaub, M., O. Gimsenez, A. Sierro, R. Arlettaz. 2007. Use of integrated modeling to enhance estimates of population dynamics obtained from limited data. Conservation Biology 21:945-955.

Smith, G. W. 1995. A critical review of the aerial and ground surveys of breeding waterfowl in North America. Biological Science Report 5, National Biological Service, Washington, D.C., USA.

U.S. Department of the Interior. 2013. Final supplemental environmental impact statement: issuance of annual regulations permitting the hunting of migratory birds. U.S. Fish and Wildlife Service, Washington, D.C. 418pp.

U.S. Fish and Wildlife Service. 2019. Adaptive Harvest Management: 2020 Hunting Season. U.S. Department of Interior, Washington, D.C. 72 pp.

Vehtari, A., A. Gelman, and J. Gabry. 2017. Practical Bayesian model evaluation using leave-one-out cross-validation and WAIC. Statistics and computing 27:1413–1432.

Watanabe, S. 2010. Asymptotic equivalence of Bayes cross validation and widely applicable information criterion in singular learning theory. Journal of Machine Learning Research 11:3571-3594.

Zimmerman, G. S., J. R. Sauer, W. A. Link, and M. Otto. 2012. Composite analysis of black duck breeding population surveys in Eastern North America. Journal of Wildlife Management 76:1165–1176.

Tables

Table 1. Definition and results of testing for functional form of the annual survival sub-model of eastern mallards. Testing was to inform the best model for use in an integrated population model. Functional form was tested using Watanabe-Akaike information criteria (WAIC).

Description	Annual Survival	WAIC	Difference from top model
Additivity on annual survival	$S_{t,ch} = \min\left(a_{0,ch}\left(1-a_{1,ch}K_{t,ch}\right), 1-K_{t,ch}\right)$	480448.5	30.3
Common linear trend	$S_{t,ch} = \min\left(a_{0,ch}\left(1-a_{1,ch}K_{t,ch}\right), 1-K_{t,ch}\right) - a_3 t$	480434.6	16.4
Age-based linear trend	$S_{t,ch} = \min\left(a_{0,ch}\left(1-a_{1,ch}K_{t,ch}\right), 1-K_{t,ch}\right) - a_{3\_A} t$	480419.6	1.4
Juvenile-only linear trend	$S_{t,ch} = \min\left(a_{0,ch}\left(1-a_{1,ch}K_{t,ch}\right), 1-K_{t,ch}\right) - I\left[A=j\right] a_3 t$	480418.2	0
Juvenile-only hockey-stick trend	$S_{t,ch} = \min\left(a_{0,ch}\left(1-a_{1,ch}K_{t,ch}\right), 1-K_{t,ch}\right) - I\left[A=j\right] a_3 \min\left(t, t_{th}\right)$	480418.7	0.5

Table 2. Fit statistics for the various sub-models of an eastern mallard integrated population model. Sub-models included pre-season (Pre) and post-season (Post) banding models of survival and harvest rate for four cohorts (adult male [AM], adult female [AF], juvenile male [JM], and juvenile female [JF]), age-ratios using hunter surveys (Wings), and a state-space model of abundance (BPOP). Measures of fit included Bayesian p-values and $\hat{c}$. Bayesian p-values close to 0 or 1 suggest lack of fit and when $\hat{c}$ is greater than 1, it suggests overdispersion of the data compared to the model.

Sub-model	Bayesian p-value	$\hat{c}$
Pre AM	0.002	1.338
Pre AF	0.002	1.372
Pre JM	0	1.669
Pre JF	0	1.565
Post AM	0.319	1.107
Post AF	0.631	0.955
Post JM	0.001	1.729
Post JF	0.001	1.832
Wings	0.311	1.389
BPOP	0.8	0.779

Table 3. Cohort-specific posterior median estimates of survival (adult male [S_{AM}], adult female [S_{AF}], juvenile male [S_{JM}], and juvenile female [S_{JF}]) and harvest (adult male [h_{AM}], adult female [h_{AF}], juvenile male [h_{JM}], and juvenile female [h_{JF}]) rates and annual age-ratios (juvenile females per adult female) from an eastern mallard integrated population model.

Year	S_{AM}	S_{AF}	S_{JM}	S_{JF}	h_{AM}	h_{AF}	h_{JM}	h_{JF}	Age-ratio
1998	0.643	0.530	0.646	0.531	0.114	0.098	0.164	0.145	0.972
1999	0.643	0.541	0.643	0.532	0.113	0.078	0.159	0.129	0.885
2000	0.636	0.531	0.623	0.509	0.125	0.096	0.211	0.173	0.744
2001	0.647	0.538	0.627	0.509	0.107	0.083	0.183	0.162	1.049
2002	0.635	0.534	0.609	0.496	0.127	0.091	0.229	0.183	0.779
2003	0.644	0.545	0.609	0.490	0.112	0.070	0.214	0.185	0.991
2004	0.644	0.536	0.598	0.490	0.113	0.087	0.238	0.174	0.973
2005	0.642	0.540	0.601	0.483	0.116	0.080	0.208	0.179	1.002
2006	0.654	0.542	0.602	0.484	0.094	0.075	0.192	0.164	1.060
2007	0.651	0.541	0.591	0.473	0.099	0.077	0.215	0.181	0.832
2008	0.644	0.540	0.580	0.462	0.112	0.080	0.237	0.196	0.912
2009	0.648	0.544	0.583	0.465	0.104	0.071	0.211	0.175	0.987
2010	0.653	0.545	0.586	0.470	0.095	0.069	0.182	0.147	0.958
2011	0.662	0.550	0.589	0.472	0.081	0.060	0.154	0.128	0.928
2012	0.656	0.550	0.577	0.460	0.091	0.061	0.179	0.148	0.914
2013	0.644	0.541	0.569	0.453	0.112	0.077	0.191	0.155	0.952
2014	0.653	0.542	0.565	0.444	0.096	0.076	0.186	0.163	0.948
2015	0.660	0.549	0.566	0.448	0.083	0.062	0.167	0.138	0.969
2016	0.653	0.544	0.557	0.440	0.096	0.072	0.181	0.148	0.926
2017	0.649	0.542	0.549	0.436	0.103	0.075	0.195	0.144	0.902
2018	0.655	0.548	0.552	0.438	0.093	0.064	0.166	0.124	0.885

Table 4. Summary statistics of simulated use of eastern mallard regulations.

	Percent time in bag limit								
Package (bag limits)	**0**	**1**	**2**	**3**	**4**	**Average fall flight**	**Percent time package is different than previous year**	**Average years between change**	**Minimum breeding abundance**
(1/2/4)	0	0	13	NA	87	1534	19	5	920
(2/3/4)	0	NA	21	0	79	1559	41	3	930
(2/4)	0	NA	13	NA	87	1535	20	5	920
	0	**1**	**2**	***4***	***6***				
(2/4/6)	0	NA	84	0	15	1642	29	4	990

Figures

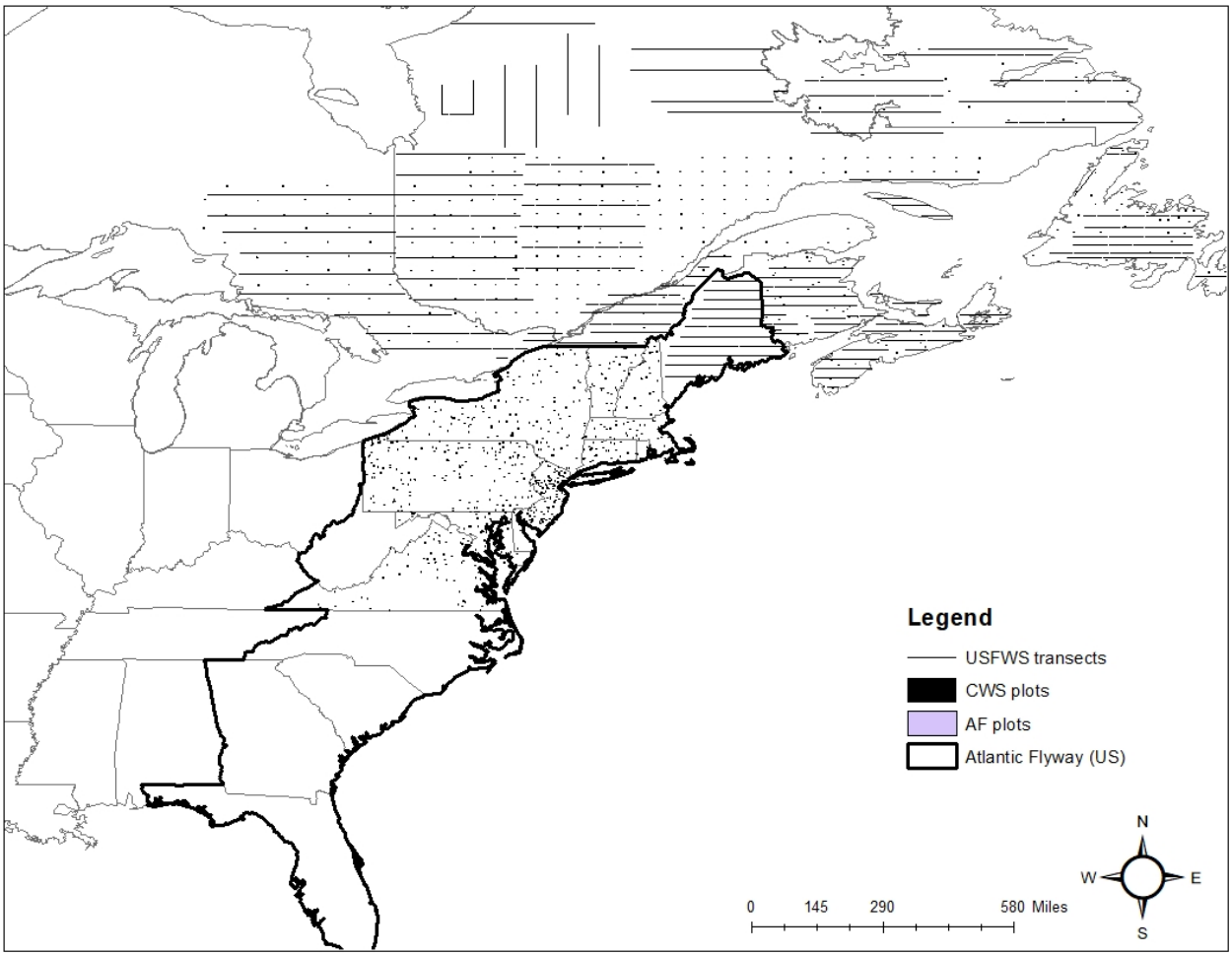

Figure 1. Map of eastern mallard range and surveys used to estimate population abundance.

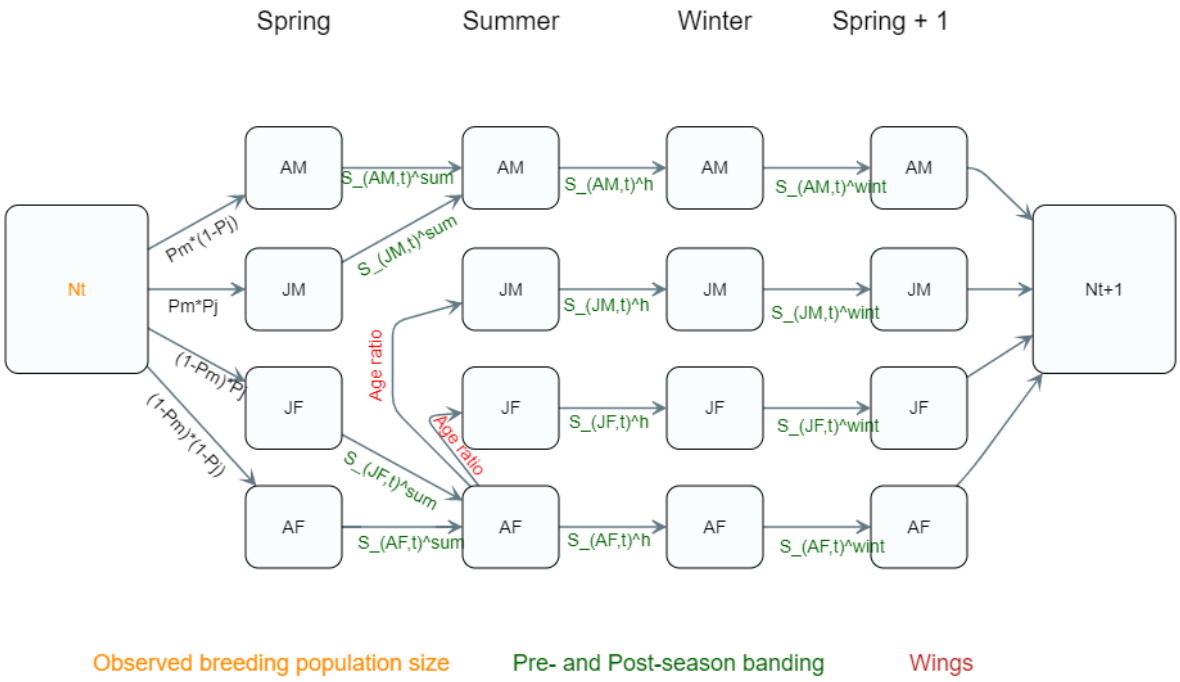

Figure 2. Annual life-cycle diagram of the integrated population model used for eastern mallards, 1998-2018. Time-step changes are cohort-specific abundance (adult male [AM], adult female [AF], juvenile male [JM], and juvenile female [JF]) and transition estimates based on data are color-coded to signify the data source.

Figure 3. Population abundance of eastern mallards based on two methods. The observed population is derived from multiple aerial surveys during the breeding season. The observed data is used in a full-annual cycle integrated population model. Posterior median estimates and 95% credible intervals of population abundance from the model are presented along with a prediction for 2019.

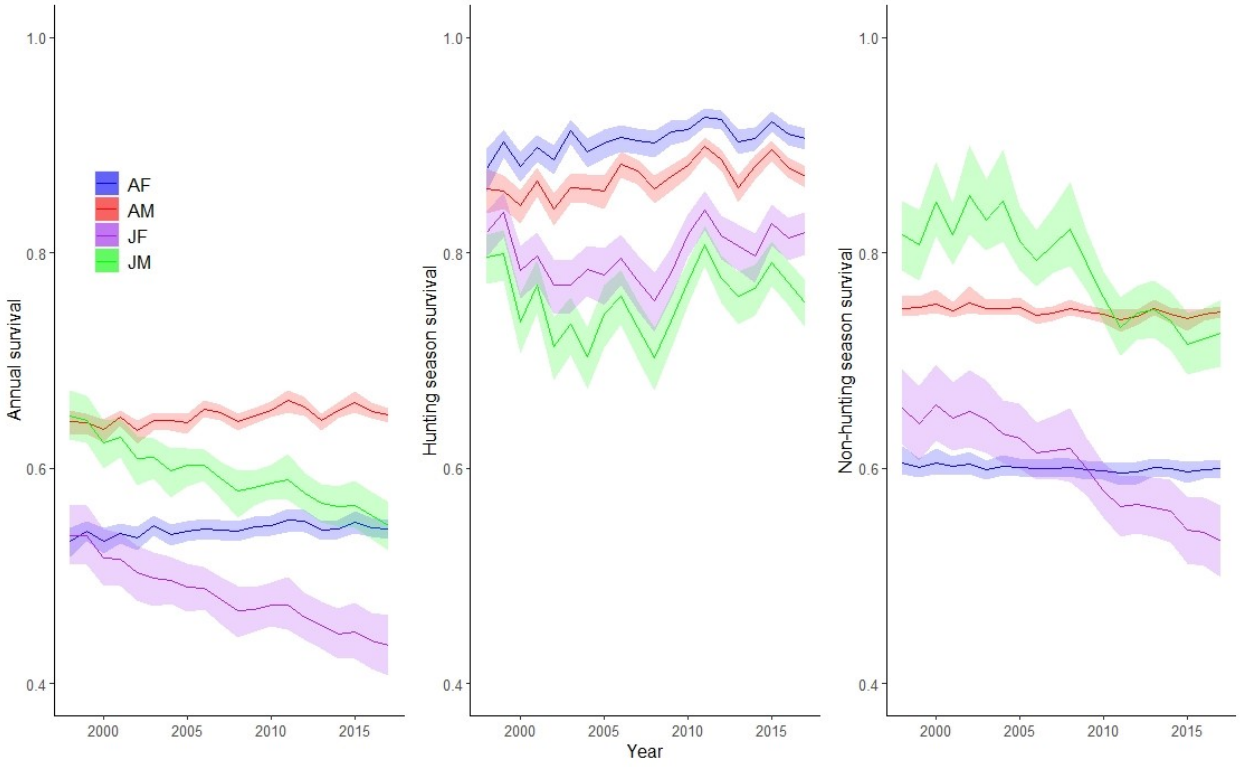

Figure 4. Plots of annual (August-August, left), hunting season (August-January, middle), and non-hunting season (February-August; right) survival of eastern mallards derived from an integrated population model, 1998-2018. Estimates are cohort-specific (adult male [AM], adult female [AF], juvenile male [JM], and juvenile female [JF]). Dark lines represent the posterior median estimate and the shading represents the 95% credible interval.

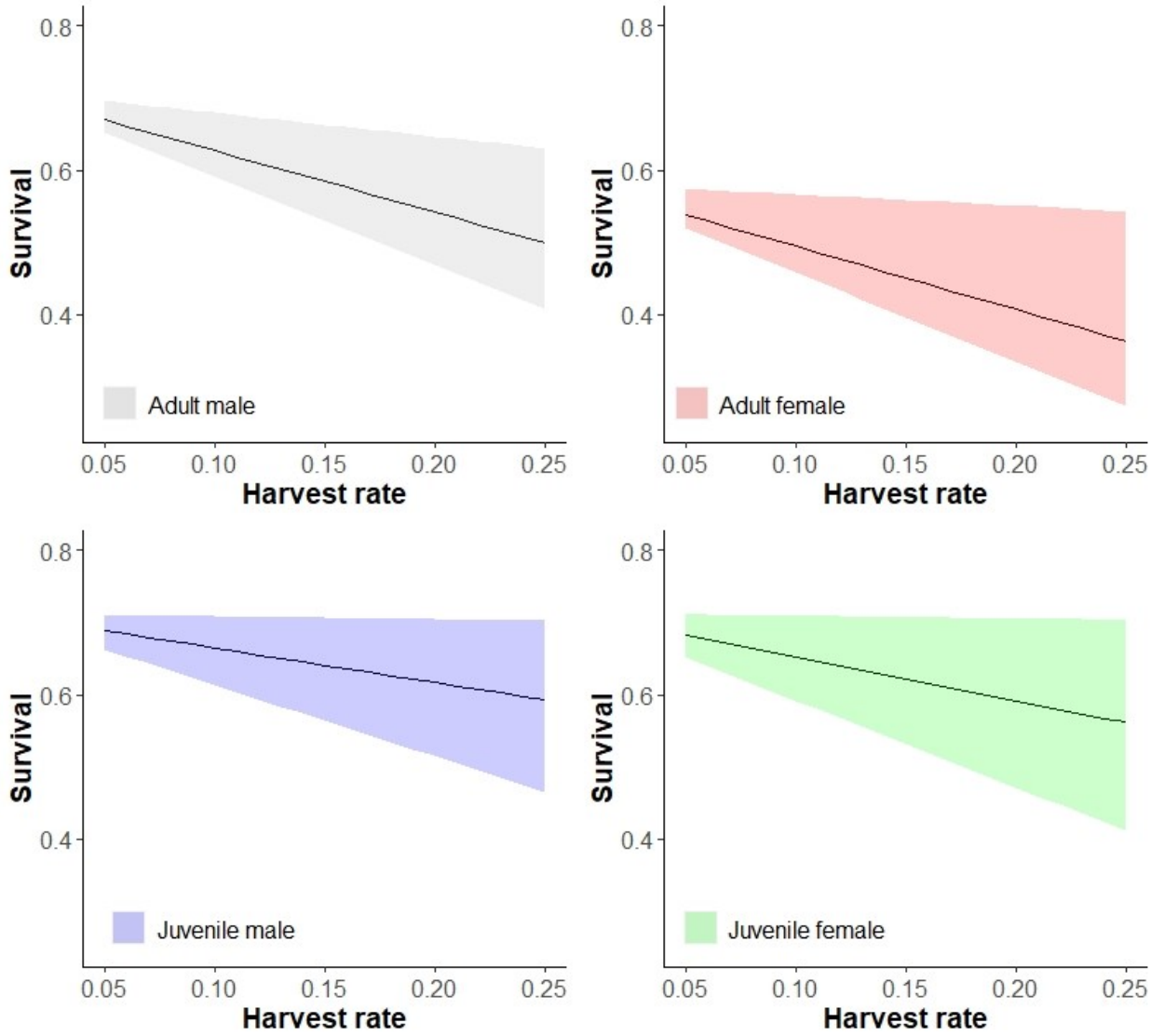

Figure 5. Estimates of cohort-specific partially compensatory harvest mortality of eastern mallards derived from an integrated population model. Dark lines represent the posterior median estimate and the shading represents the 95% credible interval.

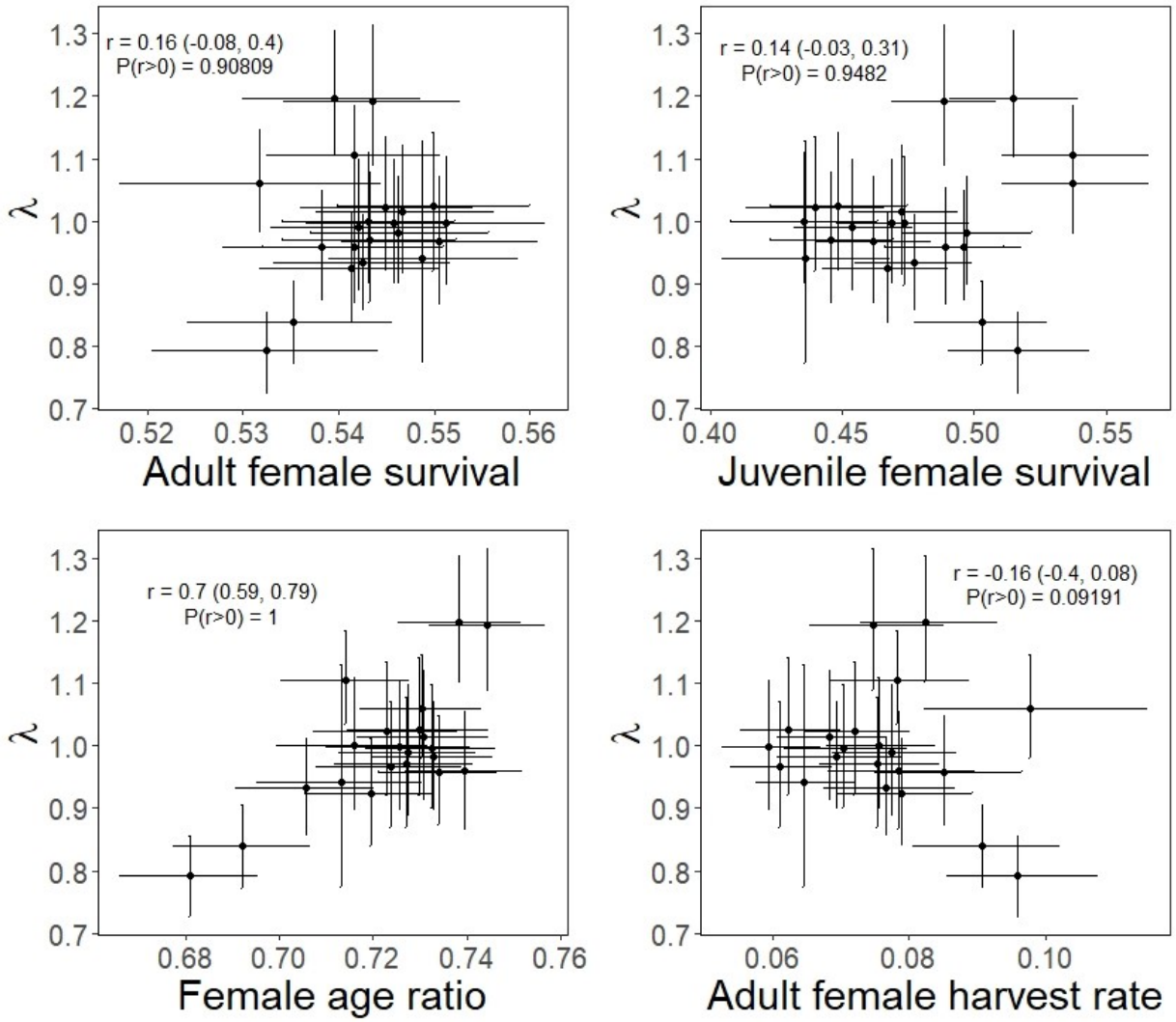

Figure 6. Estimated correlation between finite population growth rate (**λ**) of eastern mallards and: adult female (top left) and juvenile female (top right) annual survival, female fall age ratio (bottom left), and adult female harvest rate (bottom right) .

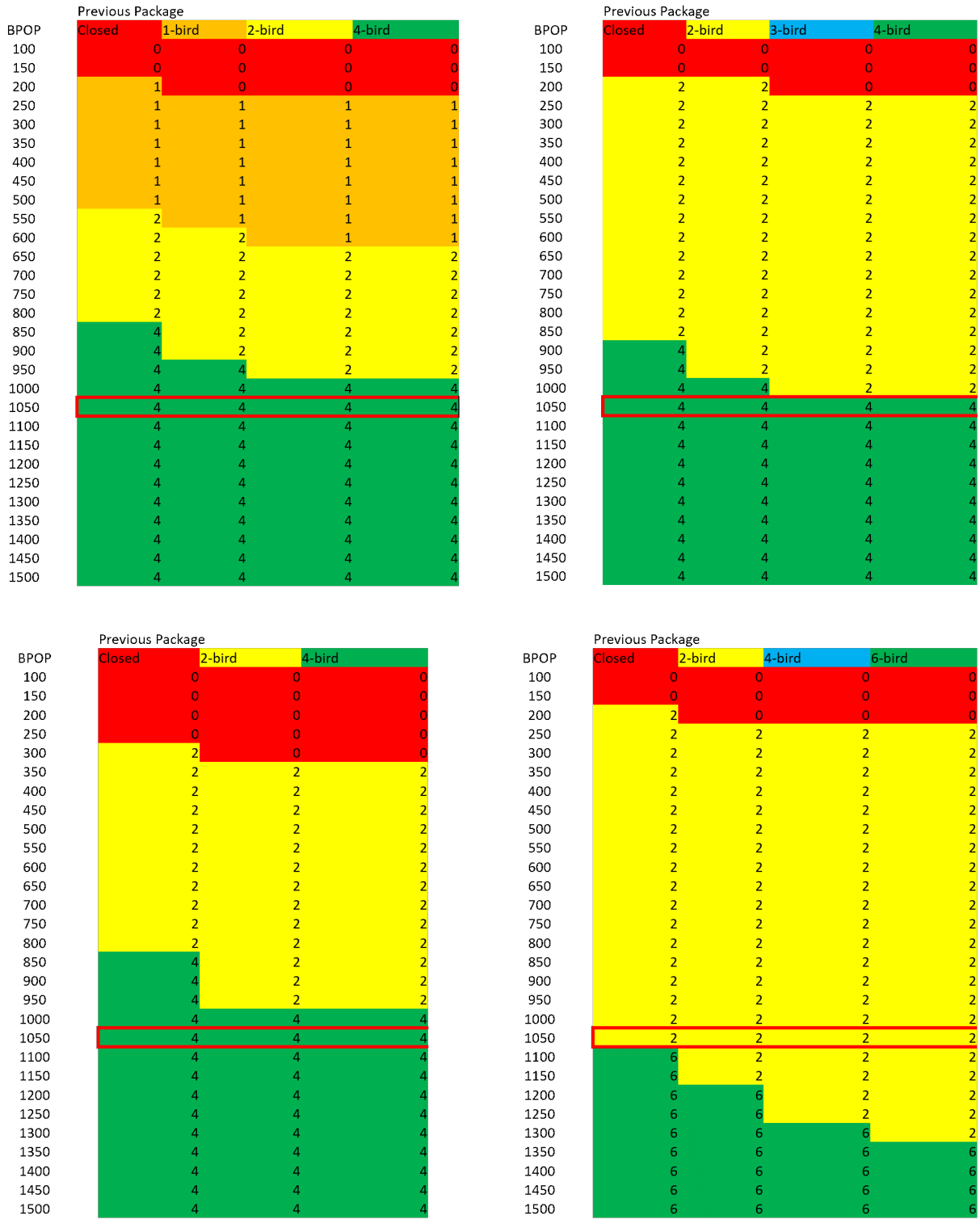

Figure 7. Depiction of optimal policy for eastern mallard harvest management based on an integrated population model and various regulations. Regulations are bag limits within a 60 day

season and are 1/2/4 (upper left), 2/3/4 (upper right), 2/4 (lower left), and 2/4/6 (lower right). Policies are a matrix of the optimal package given the breeding population abundance (BPOP; rows) and the previous year's package (columns). Red boxes highlight the row that represents the most recent observed population size.